Journal of Applied Mathematics and Physics, 2025, 13(8), 2804-2819
https://www.scirp.org/journal/jamp
ISSN Online: 2327-4379
ISSN Print: 2327-4352

Improving the Evaluation of Weak Underwater Radiated Noise Levels Using Probabilistic Geometric Spectral Subtraction

Peng Hou

Institute of Science and Technology on Underwater Test and Control, Dalian, China
Email: andyhope@126.com

How to cite this paper: Hou, P. (2025) Improving the Evaluation of Weak Underwater Radiated Noise Levels Using Probabilistic Geometric Spectral Subtraction. *Journal of Applied Mathematics and Physics*, **13**, 2804-2819.
https://doi.org/10.4236/jamp.2025.138160

Received: July 24, 2025
Accepted: August 26, 2025
Published: August 29, 2025

Abstract

Underwater radiated noise emitted by ships threatens marine ecosystems and impacts naval operations reliant on precise acoustic signatures. Measuring weak underwater radiated noise levels (URNLs) is challenged by pervasive background noise and interference, insufficient signal-plus-noise-to-noise ratio (SNNR) of a single hydrophone system, and degraded performance in near-field low-emission scenarios. In this paper, we adapt the probabilistic geometric spectral subtraction approach (PGA) previously established in speech signal processing to enhance the weak underwater radiated noise in a single hydrophone measurement. A context-aware confidence parameter for background noise estimation is embedded within the gain function, addressing the non-stationary characteristics of ship noise and dynamic underwater interference. Validated via numerical simulations and sea trials, the proposed method enhances the SNNR of the received hydrophone signal, balancing the background noise suppression and source signal preservation critical to ship radiated noise level evaluation. It improves the radiated noise level estimation reliability, effectively mitigating near-field and low-SNNR challenges, and provides a robust technical solution for weak noise level assessment, facilitating the advancement of marine acoustic measurement with engineering applicability.

Keywords

Underwater Radiated Noise Level (URNL), Background Noise, Probabilistic Geometric Spectral Subtraction Approach (PGA), Signal-Plus-Noise-to-Noise Ratio (SNNR)

1. Introduction

Underwater radiated noise emitted by ships has evolved from a niche concern in

naval signatures to a critical focus across maritime sectors, driven by escalating ecological, security, and regulatory demands [1]-[3]. Marine organisms rely on acoustic signals for survival-critical behaviors such as communication and navigation, making ship radiated noise characterized by low-frequency, broadband energy a significant threat to aquatic ecosystems [4]-[7]. Simultaneously, naval operations depend on accurate noise profiling for vessel detection and stealth technology development, while international bodies like the International Maritime Organization (IMO) increasingly mandate standardized noise measurements to enforce emission regulations [8]-[10]. These converging pressures underscore the necessity of precise evaluation of underwater radiated noise level (URNL), particularly for weak signals that carry essential information about vessel performance and environmental impact.

However, measuring weak URNLs presents formidable challenges, particularly in real-world marine environments where acoustic interference is pervasive. Underwater acoustic measurements are often plagued by high background noise from natural sources (e.g., wave action, marine life) and anthropogenic interference (e.g., other vessels, offshore activities), creating scenarios where the target signal is submerged in noise. Single-hydrophone systems, widely used for practicality, are particularly constrained by this issue: their ability to resolve weak URNL is "practically exhausted" by background interference, leading to an insufficient signal-plus-noise-to-noise ratio (SNNR) that distorts measurements [7]. This problem is exacerbated when operating in near-field conditions or for vessels with low-emission profiles, where signal attenuation and environmental distortion further degrade SNNR. Existing methods, which typically rely on uniform ship trajectories and far-field measurements, struggle to mitigate these effects, resulting in unreliable URNL estimates especially in 1/3 octave bands, the standard for noise characterization.

To address this critical gap, we draw inspiration from speech enhancement, a field with a proven track record in recovering weak signals from noisy environments. Spectral subtraction-based methods, celebrated for their low computational complexity and effective noise suppression, offer a promising solution [11]-[13]. Among these, the geometric spectral subtraction approach (GA) stands out by treating speech and noise as vectors and deriving gain functions without assuming zero cross-correlation, a key limitation of conventional approaches. However, GA's performance hinges on accurate noise estimation, a challenge in dynamic marine environments where noise characteristics fluctuate [13].

In this paper, we adapt the probabilistic geometric spectral subtraction approach (PGA) previously established in speech signal processing to enhance the weak underwater radiated noise in a single hydrophone measurement [12] [13]. While the core probabilistic framework has precedents in speech enhancement, our work incorporates marine-specific refinements: a context-aware confidence parameter for background noise estimation, embedded within the gain function, addresses the non-stationary characteristics of ship radiated noise and dynamic

interference inherent to underwater environments. This modification balances noise suppression and signal preservation (mitigating residual noise and distortion) while prioritizing spectral features critical to URNL evaluation — distinct from speech-oriented applications, which prioritize perceptual quality over acoustic metric fidelity.

Tailored explicitly for URNL assessment, the method utilizes single-hydrophone data to facilitate field deployment, accommodates near-field acoustic complexities and time-varying marine noise, and preserves 1/3 octave band characteristics which are key to standardized URNL calculation but rarely emphasized in speech-processing implementations. The efficacy is confirmed through simulations and real-ship trials. Simulations evaluate performance under lower SNNR conditions typical of weak URNL scenarios substantially harsher than those encountered in speech processing. Full scale trials, conducted across typical operational and environmental parameters (vessel speed and ambient noise), verify robustness in scenarios unique to underwater acoustics. Collectively, this adapted method advances weak URNL evaluation by improving SNNR, attenuating marine-specific interference, and retaining acoustically meaningful spectral features, enabling accurate, regulation-aligned measurements that support ecological conservation, naval innovation, and regulatory compliance.

This paper is organized as follows. Section 2 briefly addresses the URNL measurement procedure and the problem formulation. Section 3 presents the proposed method. Simulation and sea-trial results for performance validation are demonstrated in Section 4 and some concluding remarks are drawn in Section 5.

2. Problem Formulation

2.1. URNL Measurement Procedure

Figure 1 shows a typical layout for measuring the URNL of a ship. The experimental setup with a measuring hydrophone mounted in a vibration damping frame

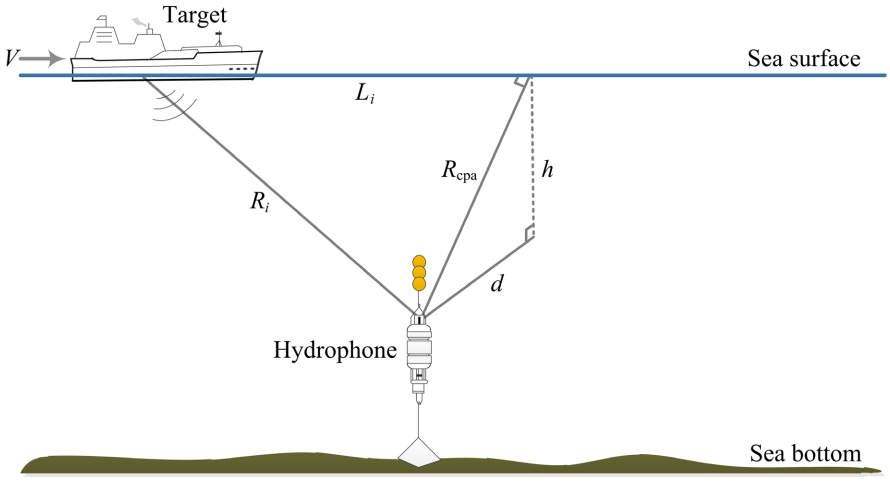

Figure 1. Layout of a typical bottom anchored setup for URNL measurement.

is deployed to the sea bed about 5 - 10 m above the base. The hydrophone signals are recorded with a sample frequency of 200 kHz. The distances between the hydrophone and the ship reference acoustic center during each measurement are determined using an underwater acoustic synchronous ranging system with a minimum period of one second [14].

During the URNL measurements, the target ship is free-sailing in a typical loading condition. Measurements are performed following the procedure described in [10] [15], and the ship is brought to a steady state about 300 m before the Closest Point of Approach (CPA) after which no changes in the machinery settings are applied and steering is kept to a minimum. Several runs are required to perform for each condition to mitigate the variation during an underwater measurement campaign [6].

Then, measured underwater radiated noise spectra are converted to URNLs using a reference pressure of 1 μPa and a constant 1 Hz bandwidth. The results are then converted to 1/3 octave bandwidth and the results of all runs are then averaged for each condition after undergoing an adjustment phase of background noise, sensitivity and distance. The measured URNLs are strongly dependent on the actual distances between the target ship and the receiving hydrophone. At short distances, the transmission loss can be approximated by a spherical spreading law and frequency-dependent absorption [5] [14] [15].

2.2. Signal Model and Main Issue

For most of the full scale experiments of URNL measurement, the recorded hydrophone signals are corrupted by the ocean background noise and interferences, which causes a hard detection of radiated noise sources and leads to a performance decrease of noise measuring and analyzing systems.

Let us consider an additive mixture of a single-channel hydrophone signal $y(n)$,

$$y(n) = s(n) + w(n), \tag{1}$$

where $s(n)$ is the source signal of interest, $w(n)$ is ocean background noise, and n is the discrete-time index. In most of the test campaigns, relatively quiet water areas will be chosen and the background noise does not include obvious interference noise sources [14]. The background noise signal is usually assumed to be additive and statistically independent from the source signal.

A set of background noise data is to be collected at the beginning and at the end of each measurement run, which enables the comparison of the broadband sound pressure level (SPL) or overall sound level radiated from the ship under test to the background noise level during the period of the measurement. Define the signal-plus-noise-to-noise ratio (SNNR) as [10],

$$\Delta L = 10\log_{10}\left(p_{s+n}^2 / p_n^2\right), \tag{2}$$

where p_{s+n} is the total underwater sound pressure received at the hydrophone, in μPa, and p_n is the sound pressure of the background noise received at the hydrophone. **Figure 2** shows the passing characteristic curves of a moving ship

with different ΔL, which demonstrate the dependence of the averaged squared magnitude value of the sound pressure on time in 1/3 octave bands. It is worth noting that the measured URNL results might be considered as invalid data for the case of $\Delta L < 3$ dB [9] [10], which is currently the common situation for a relative high background noise level.

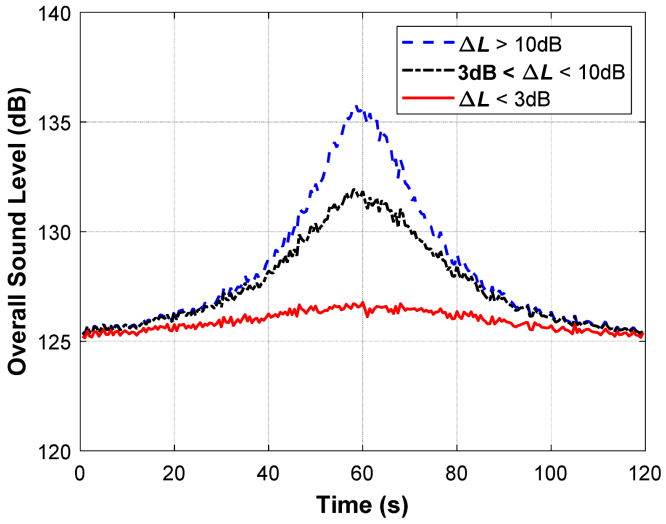

Figure 2. The passing characteristic curves of a moving ship with ΔL = 10.5, 6.6 and 1.6 dB respectively.

In this paper, we refer to this situation (*i.e.* $\Delta L < 3$ dB) as "the weak underwater radiated noise levels", which serves as the main issue we aim to address. Inspired by the speech enhancement, we try to use the idea of spectral subtraction to enhance the ship radiated noise signal with low ΔL, so as to improve the evaluation capability of weak URNLs in a high background noise environment. The task is then to suppress the background noise $w(n)$ in the best possible way without distorting the source signal $s(n)$ resulting in the following critical spectral representation of $y(n)$.

Taking the short-time Discrete Fourier Transform (DFT) of $y(n)$ for frame λ, we get

$$Y^{\lambda}(\omega_k) = S^{\lambda}(\omega_k) + W^{\lambda}(\omega_k), \tag{3}$$

where $S^{\lambda}(\omega_k)$ and $W^{\lambda}(\omega_k)$ are the DFT coefficients of $s(n)$ and $w(n)$ respectively, $\omega_k = 2\pi k/N$, $k = 0, 1, 2, \ldots, N-1$, N is the frame length in samples, λ is the time frame index, $\lambda = 1, \ldots, \Lambda$. Thus, from the basic rule of spectral subtraction, the estimate of the source signal power spectrum, denoted as $\left|S^{\lambda}(\omega_k)\right|^2$, can be obtained by

$$\left|S^{\lambda}(\omega_k)\right|^2 = \left|Y^{\lambda}(\omega_k)\right|^2 - \left|W^{\lambda}(\omega_k)\right|^2. \tag{4}$$

The above equation describes the so called *spectral subtraction* algorithm. Low computational complexity with better noise suppression ability is the main charm of the spectral subtraction-based methods [11]. However, most of the methods

assume that the noise and source signal are uncorrelated in the short frame and the noise estimate is accurate, which is not true for most of the practical scenarios. In [12], a probabilistic geometric spectral subtraction was proposed, where a confidence parameter of noise estimation is introduced in the gain function to prevent the source distortion and noise residual in the enhanced signal. Tips for the proposed method will be discussed in the sequel.

3. Proposed Method

For the problem of URNL measurement, the estimation of the noise spectrum from the pre-collected background noise data is relatively straightforward. However, the measured background noise changes dynamically with sea areas and time periods, resulting in poor stability [4] [16]. Furthermore, ideal interference-free measurement points are hard to select due to terrain and hydrological conditions, and the noise from the target ship and other industrial activities may overlap spectrally with background noise, with blurred boundaries. All of these will make the separation between background noise and complex environmental interference difficult. In this paper, we adapt the PGA to the noise estimation and enhancement of weak received hydrophone signals.

Geometrically, the Equation (3) can be expressed in polar form as

$$a_Y^{\lambda}\left(\omega_k\right)e^{\mathrm{j}\theta_Y^{\lambda}\left(\omega_k\right)}=a_S^{\lambda}\left(\omega_k\right)e^{\mathrm{j}\theta_S^{\lambda}\left(\omega_k\right)}+\rho^{\lambda}a_W^{\lambda}\left(\omega_k\right)e^{\mathrm{j}\theta_W^{\lambda}\left(\omega_k\right)}, \tag{5}$$

where $a_Y^{\lambda}\left(\omega_k\right)$, $a_S^{\lambda}\left(\omega_k\right)$, $a_W^{\lambda}\left(\omega_k\right)$ are the magnitudes and $\theta_Y^{\lambda}\left(\omega_k\right)$, $\theta_S^{\lambda}\left(\omega_k\right)$, $\theta_W^{\lambda}\left(\omega_k\right)$ are the phases of the noisy hydrophone signal, source signal and background noise spectra respectively, ρ^{λ} is a special variable known as the confidence parameter of noise estimation. The estimate of Equation (4) can be written in the following form [12]:

$$\left|\hat{S}^{\lambda}\left(\omega_k\right)\right|^2=\left|H_{PGA}^{\lambda}\left(\omega_k\right)\right|^2\left|Y^{\lambda}\left(\omega_k\right)\right|^2, \tag{6}$$

where

$$H_{PGA}^{\lambda}\left(\omega_k\right)=\sqrt{\frac{1-\left(\dfrac{\gamma+\rho^2-\xi}{2\sqrt{\gamma}\rho}\right)^2}{1-\left(\dfrac{\gamma-\rho^2-\xi}{2\sqrt{\xi}\rho}\right)^2}}, \tag{7}$$

is the gain function of probabilistic geometric approach for the λ^{th} frame. The parameters γ and ξ are the instantaneous a posterior and a priori SNRs respectively which are defined as follows:

$$\gamma\triangleq\frac{a_Y^2\left(\omega_k\right)}{a_W^2\left(\omega_k\right)},\quad \xi\triangleq\frac{a_S^2\left(\omega_k\right)}{a_W^2\left(\omega_k\right)}. \tag{8}$$

Therefore, by increasing or decreasing $H_{PGA}^{\lambda}\left(\omega_k\right)$ in Equation (7), the source distortion and noise residual in the received hydrophone signal is prevented. The magnitude of the received hydrophone signal spectrum is then compensated

based on this confidence parameter.

The confidence parameter ρ is introduced in the gain function to prevent subtraction of the overestimated and underestimated noise. Inspired by [13], the confidence parameter ρ at the λ^{th} frame can be determined by

$$\rho^{\lambda}(\omega_k) = \sqrt{1 - P_{\text{local}}^{\lambda}(\omega_k) P_{\text{global}}^{\lambda}(\omega_k) P_{\text{frame}}^{\lambda}}, \tag{9}$$

where $P_{\text{local}}^{\lambda}(\omega_k)$ and $P_{\text{global}}^{\lambda}(\omega_k)$ are determined from the following equation,

$$P_{\psi}^{\lambda}(\omega_k) = \begin{cases} 0, & \text{if } \zeta_{\psi}^{\lambda}(\omega_k) \le \zeta_{\min}, \\ 1, & \text{if } \zeta_{\psi}^{\lambda}(\omega_k) \ge \zeta_{\max}, \\ \dfrac{\log\left(\zeta_{\psi}^{\lambda}(\omega_k)/\zeta_{\min}\right)}{\log\left(\zeta_{\max}/\zeta_{\min}\right)}, & \text{otherewise}, \end{cases} \tag{10}$$

where the subscript ψ denotes either local or global, and $\zeta_{\psi}^{\lambda}(\omega_k)$ represents a recursive average of the a priori SNR, $\zeta_{\min}$ and $\zeta_{\max}$ are empirical constants maximized to attenuate noise. By applying local and global averaging windows in the frequency domain, we obtain, respectively, local and global averages of the a priori SNR:

$$\zeta_{\psi}^{\lambda}(\omega_k) = \sum_{i=-W_{\psi}}^{i=W_{\psi}} h_{\psi}^{\lambda}(\omega_k) \zeta^{\lambda}(\omega_k - \omega_i), \tag{11}$$

where h_{ψ}^{λ} is the normalized window of size $2W_{\psi}+1$, $\zeta_{\psi}^{\lambda}(\omega_k)$ is the recursive average of the a priori SNR with a time constant β,

$$\zeta^{\lambda}(\omega_k) = \beta \zeta^{\lambda-1}(\omega_k) + (1-\beta)\eta^{\lambda-1}(\omega_k), \tag{12}$$

where $\eta^{\lambda-1}(\omega_k)$ is the estimated a priori SNR.

In order to further attenuate noise, the parameter $P_{\text{frame}}^{\lambda}$ is determined as

$$P_{\text{frame}}^{\lambda} = \begin{cases} 0, & \text{if } \zeta_{\text{frame}}^{\lambda} \le \zeta_{\min}, \\ 1, & \text{if } \zeta_{\text{frame}}^{\lambda} \ge \zeta_{\min} \text{and } \zeta_{\text{frame}}^{\lambda} \ge \zeta_{\text{frame}}^{\lambda-1}, \\ \mu^{\lambda}, & \text{otherewise}, \end{cases} \tag{13}$$

where

$$\mu^{\lambda} = \begin{cases} 0, & \text{if } \zeta_{\text{frame}}^{\lambda} \le \zeta_{\text{peak}}^{\lambda} \zeta_{\min}, \\ 1, & \text{if } \zeta_{\text{frame}}^{\lambda} \ge \zeta_{\text{peak}}^{\lambda} \zeta_{\max}, \\ \dfrac{\log\left(\zeta_{\text{frame}}^{\lambda} \zeta_{\text{peak}}^{\lambda}/\zeta_{\min}\right)}{\log\left(\zeta_{\max}/\zeta_{\min}\right)}, & \text{otherewise}, \end{cases} \tag{14}$$

represents a soft transition from "interferences" to "background noise", $\zeta_{\min}$, $\zeta_{\max}$ and ζ_{peak} are empirical constants. $\zeta_{\text{frame}}^{\lambda}$ is an averaging of $\zeta^{\lambda}(\omega_k)$ over certain frequency band with confined peak value $\zeta_{\text{peak}}^{\lambda}$, given by

$$\zeta_{\text{frame}}^{\lambda} = \frac{1}{M} \sum_{k=0}^{M-1} \zeta^{\lambda}(\omega_k). \tag{15}$$

Finally, the enhanced hydrophone signal is obtained by computing the inverse Fourier Transform (IDFT) of $\left|\hat{S}^{\lambda}(\omega_k)\right|$ using the phase of the received

hydrophone signal, that can be written as

$$\hat{s}^{\lambda}(n) = \mathrm{Re}\left[\mathrm{IDFT}\left(\left|\hat{S}^{\lambda}(\omega_k)\right| e^{j\theta_Y^{\lambda}\omega_k}\right)\right], \tag{16}$$

where $\mathrm{Re}[\cdot]$ finds the real part of each element in it. From the post-processing data, the 1/3 octave band SPLs and URNLs are determined.

4. Results and Discussion

4.1. Simulation Validation

Numerical simulations were initially performed to evaluate the performance of the proposed method under a typical full-scale ship testing scenario. As is well-established, the underwater noise spectrum radiated by a vessel results from the combined action of multiple noise sources, such as propulsion machinery and various pumps. Divergent noise generation mechanisms yield distinct spectral characteristics of the radiated noise. Generally, the ship-radiated noise spectrum encompasses both broadband continuous components and narrowband line spectra. We approximated the broadband components of the URNLs using Ross' speed-dependent spectrum model [2], to which tonal components representing propeller blade rate harmonics, diesel engine firing harmonics, etc., were superimposed. The amplitudes of these tonal components were scaled such that the highest tones exceeded the broadband spectrum by approximately 10 - 15 dB. The ambient background noise was derived from actual marine environments, featuring a typical kurtosis value of 3.06, consistent with the representative white-Gaussian noise profile [17].

In practice, surface ships emit varying noise levels contingent on their operational conditions. Appropriate hydrophone configurations must be selected to ensure reproducible URNL measurements. However, determining optimal operational parameters and target-receiver geometries to achieve robust and consistent URNL measurements lies beyond the scope of this paper. Our focus is on generating controlled hydrophone signals with weak URNLs representative of a single ship navigating in open water.

For this study, radiated noise simulations were conducted for a vessel transiting a straight path over a hydrophone at a speed of 10 knots. The total traversing distance was assumed to be 600 m, extending 300 m on either side of a hypothetical hydrophone deployed at a depth of 40 m. This configuration resulted in a 116-second radiated noise dataset. Hydrophone signals containing frequencies up to 5 kHz with varying URNLs were finally obtained by adjusting the CPA distances [see **Figure 1**].

Figure 3 illustrates the time-frequency characteristics of the radiated noise signal from a typical moving vessel. As evident in **Figure 3(a)**, the radiated noise exhibits distinct line spectral features primarily originating from the propeller blade rate and its harmonic series, such as 11 Hz (blade rate) and 55 Hz (fifth harmonic), corresponding to a 4-blade propeller rotating at approximately 165

RPM.

Figure 4 presents the results of normalized URNL under SNNRs of 6 dB, 3 dB, 2 dB and 1 dB respectively. For each SNNR condition, the comparison of three types of results, namely the received noisy hydrophone signal, the enhanced hydrophone signal and the real source signal, is provided. The issue of background correction is not considered here for the time being. It is evident that by implementing the proposed method the SNNR of ship radiated noise is further enhanced with all post-processing SNNRs exceeding 3 dB.

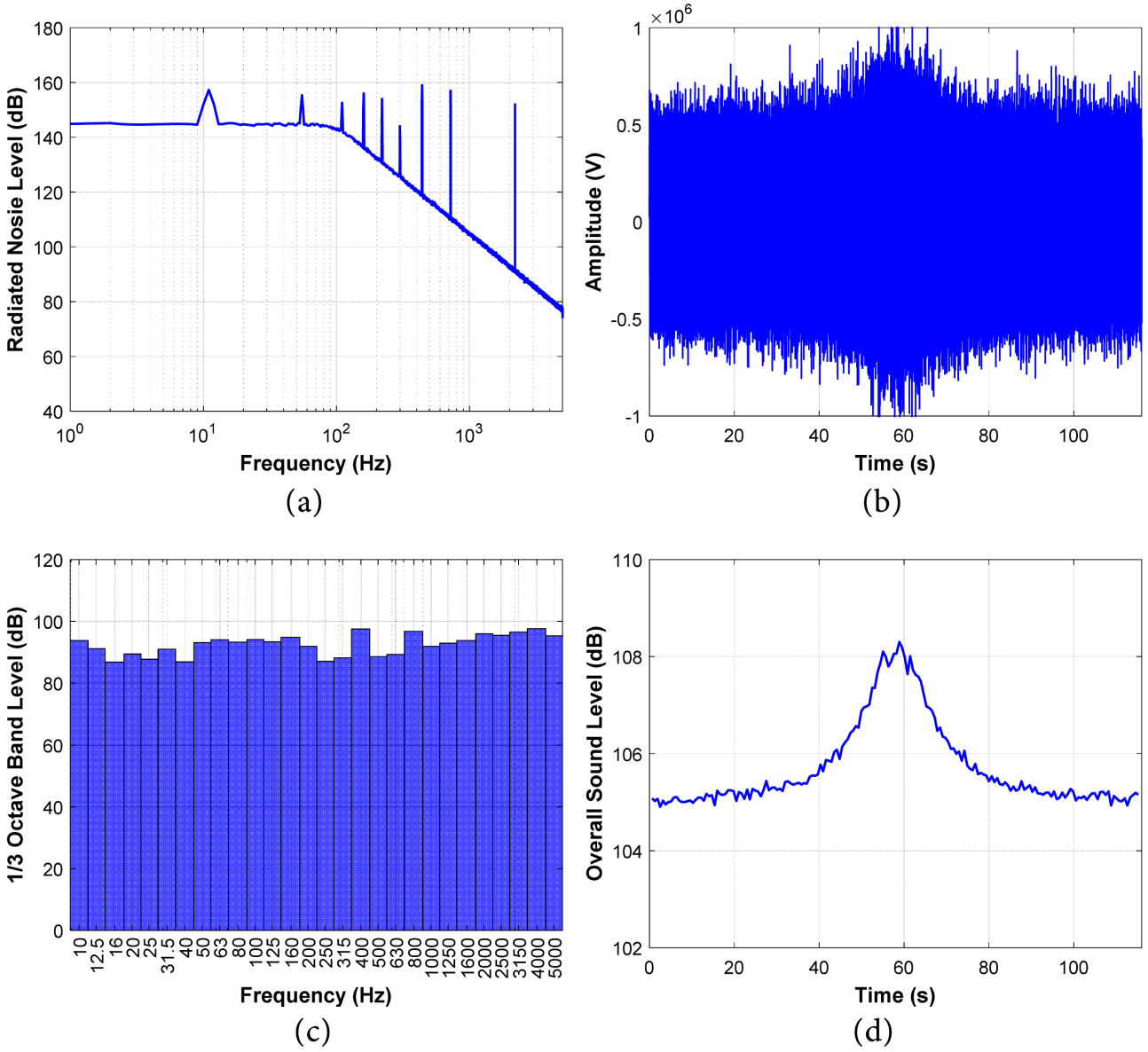

Figure 3. Typical characteristics of the simulated radiated noise emitted by a moving vessel for (a) radiated noise level, (b) time series signal, (c) 1/3 octave band levels, and (d) passing characteristic curves.

As shown in **Figure 4**, the simulation results indicate that the URNLs of the ship are consistently overestimated in all SNNR scenarios. As the SNNR

decreases, the estimation deviation of the URNL of the enhanced hydrophone signal relative (green dash-dot line) to the source signal (red solid line) gradually grows. Specifically, the deviations are 0.4 dB at an SNNR of 6 dB, 1 dB at 3 dB, 1.5 dB at 2 dB, and 2.7 dB at 1 dB. For the case of SNNR lower than 1 dB (e.g., 0 dB), a relatively large deviation exceeding 3 dB will arise, which is unacceptable in such cases.

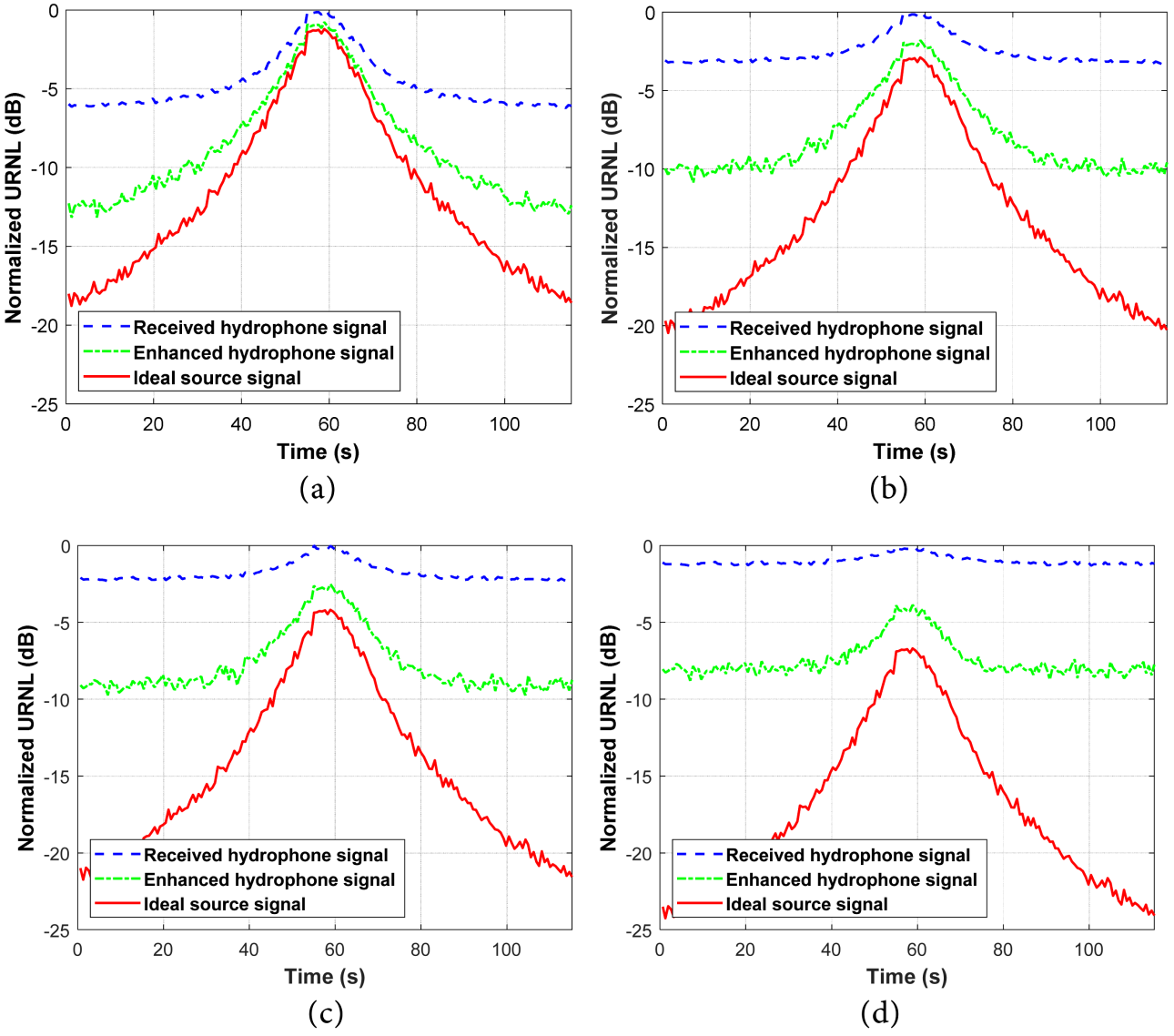

Figure 4. Normalized dependences of traffic boat URNL on time for (a) $\Delta L = 6.0$ dB, (b) $\Delta L = 3.0$ dB, (c) $\Delta L = 2.0$ dB, and (d) $\Delta L = 1.0$ dB.

According to the spectral characteristics of ship radiated noise depicted in **Figure 3**, **Figure 5** illustrates the results of normalized 1/3 octave band SPL at the typical center frequencies of 100 Hz, 160 Hz, 400 Hz and 800 Hz, respectively. Similarly, in each case, the results of three types of signals, namely the received noisy hydrophone signal, the enhanced hydrophone signal and the real source

signal, are compared.

It can be seen that the proposed method can be used to enhance the narrowband signals. However, this improvement is not absolute and is constrained by the stability of the line spectra of ship radiated noise. When the line spectrum characteristics remain relatively stable during the ship's maneuvering operations, the passing characteristic curve is typically smooth, leading to a relatively satisfactory noise suppression effect. Conversely, when the line spectrum characteristics exhibit fluctuations, the passing characteristic curve also displays certain random fluctuation features as shown in **Figure 5(b)**. In general, as the SNNR decreases, the estimation deviation of the URNL of the enhanced hydrophone signal relative (green dash-dot line) to the source signal (red solid line) gradually grows. Specifically, the deviations are 0.5 dB at a frequency of 100 Hz, 1.3 dB at 160 Hz, 0.6 dB at 400 Hz, and 1.5 dB at 800 Hz. The simulation results also indicate that in the vicinity of strong line spectra, such as 11 Hz and 55 Hz [see **Figure 3(a)**], the

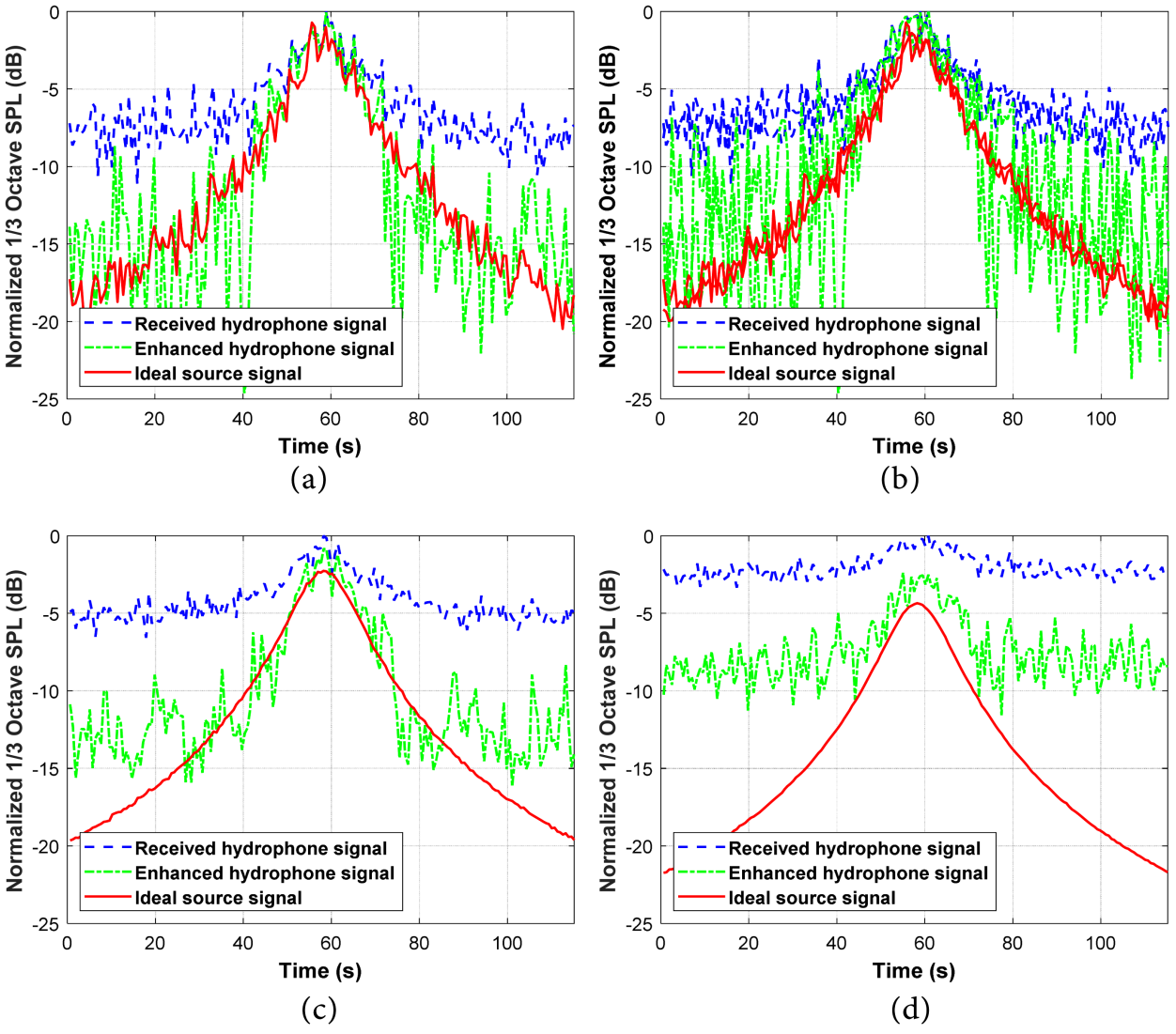

Figure 5. Normalized 1/3 octave band SPL at the typical centre frequencies for (a) 100 Hz, (b) 160 Hz, (c) 400 Hz and (d) 800 Hz.

estimation deviation is within 0.5 dB.

4.2. On-Site Measurement

The on-site measurements were performed utilizing a small traffic boat, the BEIJIAO-01. This ship is 45 m overall length, with a maximum beam of 8.4 m, a draft of 3 m, and a displacement of 438 tons. BEIJIAO-01 is propelled by two five-bladed propellers with a maximum speed of 16 knots.

To secure measurement results across varying distances and enhance testing efficiency, four identical bottom anchored setups (submerged buoy, see **Figure 1**) were deployed at a depth of 35 m, each completely self-contained with an operational duration exceeding 72 hours. Each setup continuously recorded data from hydrophone channel onto an internal hard drive with a sample frequency of 200 kHz and a 24-bit dynamic range. Subsequently, the SPLs of full-scale ship in 1/3 octave bands were determined, and a background noise correction was then applied.

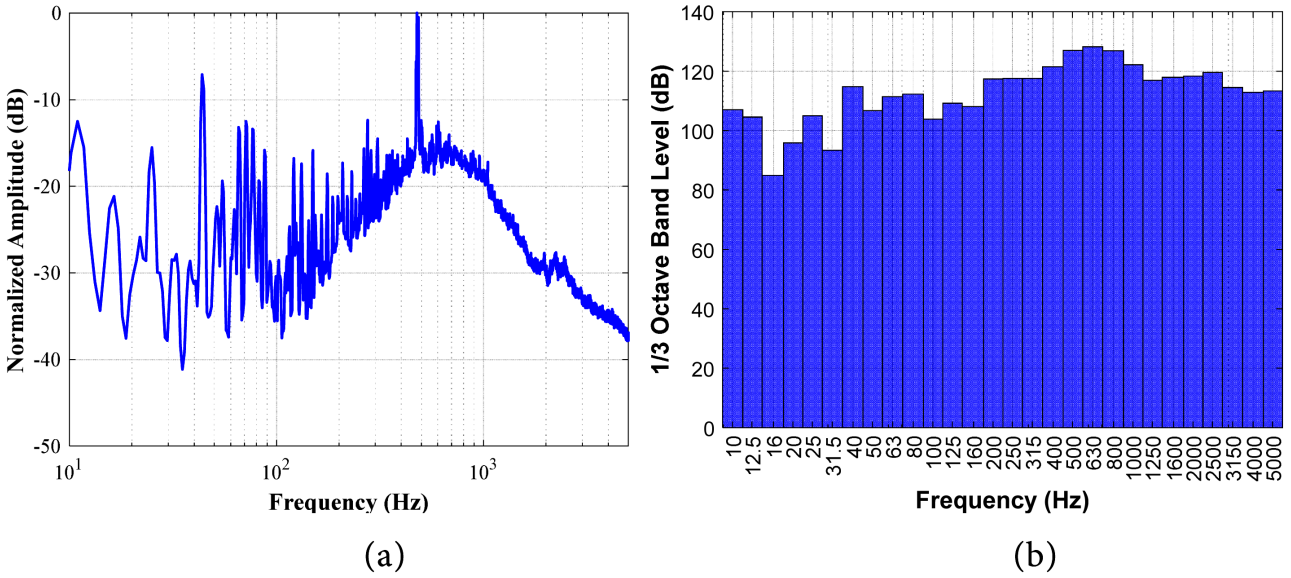

Figure 6. Radiated noise spectral characteristics of BEIJIAO-01 from one bottom anchored setup during a straight, constant-speed run at 6 knots. (a) The line spectrum. (b) The 1/3 octave band levels.

Figure 6 demonstrates the spectral characteristics of the radiated noise for BEIJIAO-01 transiting a straight path over one measurement setup at a speed of about 6 knots. As shown in **Figure 4(a)**, the main radiated noise spectra of the traffic boat BEIJIAO-01 are concentrated in the low-to-medium frequency range below 500 Hz. There are multiple line spectra below 100 Hz, such as 11 Hz, 15.6 Hz, 25 Hz, 43.7 Hz, 65.6 Hz, 71 Hz, 76.5 Hz, as well as the medium frequency components of 275 Hz, 476 Hz and 484 Hz. These line spectra may arise from multiple mechanisms. The relatively low-frequency line spectra (below 100 Hz) are likely generated by the rotating components of the boat's propulsion system, such as the shaft frequency and its harmonics produced by the rotation of the propeller shaft [1] [14]. The medium-frequency line spectra (like 275 Hz) may be related to the

blade-passing frequency of the propeller and its higher-order harmonics. Additionally, mechanical resonances in the hull or structural components of the boat can amplify specific frequencies contributing to the observed line spectra in the noise signature.

Figure 7 presents the results of normalized URNL under four abeam CPA distances (66.43 m, 75.26 m, 84.27 m and 116.43 m). It is evident that the SNNR of the ship radiated noise has been significantly improved by applying the method proposed in this paper. The processing results for different abeam distances indicate that the spectra of the enhanced hydrophone signal exhibit good consistency with that of the original noisy hydrophone signal around the time of CPA. Regrettably, we have not yet obtained verification of ship radiated noise under lower SNNR conditions, which will be the focus of our subsequent work. However, the above results demonstrate that our proposed method has significant engineering

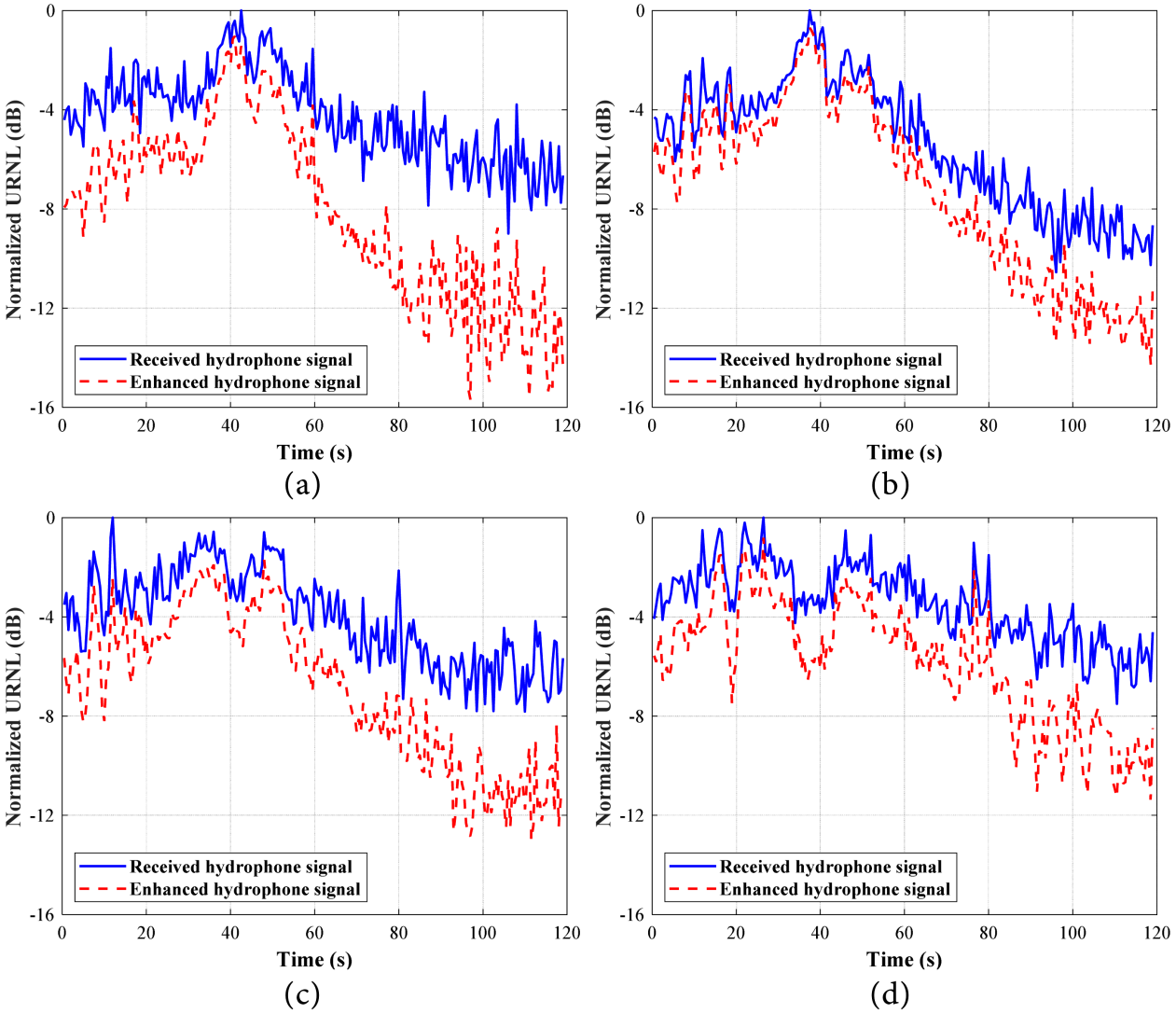

Figure 7. Normalized dependences of traffic boat URNL on time from four bottom anchored setups with (a) R_{cpa} = 66.43 m, (b) R_{cpa} = 75.26 m, (c) R_{cpa} = 84.27 m, and (d) R_{cpa} = 116.43 m.

applicability and can serve as a potential and reliable technical means for evaluating the weak URNL.

5. Conclusions

Ship-radiated underwater noise poses dual challenges: it endangers marine ecosystems reliant on acoustic communication and hinders naval operations that demand precise measurement of URNL. Conventional methods struggle to tackle the complexities of marine environments, particularly when dealing with weak signals. We have adapted a probabilistically modified geometric spectral subtraction method, previously designed for speech signal processing, to enhance weak underwater radiated noise in a single hydrophone measurement. The method incorporates marine-specific refinements, a context-aware confidence parameter for background noise estimation embedded within the gain function, to balance the background noise suppression and source signal preservation. Numerical simulations and full scale trials confirm the method's efficacy with post-processing SNNRs far exceeding 3 dB in most scenarios.

Compared with the noise within speech processing, the sources, frequency ranges, waveform characteristics and propagation properties of marine environmental noise and interference in the assessment of ship radiated noise are all distinct. Typically, the waveform of marine noise is complex and irregular, often exhibiting random and continuous characteristics. In contrast, speech noise has a certain regularity and periodicity, associated with the rhythm and tempo of human vocalization, featuring obvious syllable intervals and intonation variations. The method proposed herein adheres to the established empirical parameter-selection principles in speech noise estimation. While demonstrating significant engineering potential, optimally selecting relevant parameters and further validating under extremely low-SNNR conditions are still required. Future work will focus on adapting the method to a wider range of vessel types, integrating it with array signal processing and optimizing it for the most challenging low-SNNR marine environments, solidifying its role as a cornerstone in marine acoustic engineering.

Acknowledgements

The authors would like to thank the fellows of the Institute of Science and Technology on Underwater Test and Control for conducting the tough sea trials and providing useful experiment data in this paper.

Conflicts of Interest

The author declares no conflicts of interest regarding the publication of this paper.

References

[1] Moore, S. (2019) Acoustic Signature Control on Maritime Platforms. *Annual*

Conference of the Australian Acoustical Society 2019, Cape Schanck, 10-13 November 2019, 1-12.

[2] Gaggero, T., Rizzuto, E., Traverso, F. and Trucco, A. (2014) Comparing Ship Underwater Noise Measured at Sea with Predictions by Empirical Models. *Proceedings of the* 21*st Congress on Sound and Vibration*, Beijing, 13-17 July 2014, 1-7.

[3] Lafeber, F.H., Lloyd, T. and Bosschers, J. (2017) Validation of Underwater Radiated Noise Predictions for a Merchant Vessel Using Full-Scale Measurements. *Proceedings of the* 46*th Congress and Exposition on Noise Control Engineering*, Hong Kong, 27-30 August 2017, 3857-3866.

[4] Sakai, M., Haga, R., Tsuchiya, T., Akamatsu, T. and Umeda, N. (2023) Statistical Analysis of Measured Underwater Radiated Noise from Merchant Ships Using Ship Operational and Design Parameters. *The Journal of the Acoustical Society of America*, **154**, 1095-1105. https://doi.org/10.1121/10.0020668

[5] Trevorrow, M.V., Vasiliev, B. and Vagle, S. (2008) Directionality and Maneuvering Effects on a Surface Ship Underwater Acoustic Signature. *The Journal of the Acoustical Society of America*, **124**, 767-778. https://doi.org/10.1121/1.2939128

[6] Ainslie, M.A., Martin, S.B., Trounce, K.B., Hannay, D.E., Eickmeier, J.M., Deveau, T.J., *et al.* (2022) International Harmonization of Procedures for Measuring and Analyzing of Vessel Underwater Radiated Noise. *Marine Pollution Bulletin*, **174**, Article ID: 113124. https://doi.org/10.1016/j.marpolbul.2021.113124

[7] Orlov, D., Fiks, I., Fiks, G., Korotin, P. and Turchin, V. (2008) Adaptive Beamforming Applied to Underwater Acoustic Measurements. *The Journal of the Acoustical Society of America*, **123**, 3465-3465. https://doi.org/10.1121/1.2934326

[8] BS ISO 17208-1 (2016) Underwater Acoustics—Quantities and Procedures for deScription and Measurement of Underwater Sound from Ships—Part1: Requirements for Precision Measurements in Deep Water Used for Comparison Purposes. 3rd Edition, International Organization for Standardization.

[9] MacGillivray, A.O., Martin, S.B., Ainslie, M.A., Dolman, J.N., Li, Z. and Warner, G.A. (2023) Measuring Vessel Underwater Radiated Noise in Shallow Water. *The Journal of the Acoustical Society of America*, **153**, 1506-1524. https://doi.org/10.1121/10.0017433

[10] ABS (2025) Guide for the Classification Notation—Underwater Noise and External Airborne Noise. American Bureau of Shipping, 23-36.

[11] Lu, Y. and Loizou, P.C. (2008) A Geometric Approach to Spectral Subtraction. *Speech Communication*, **50**, 453-466. https://doi.org/10.1016/j.specom.2008.01.003

[12] Islam, M.D., Shahnaz, C., Zhu, W.P. and Ahmad, M.O. (2018) Enhancement of Noisy Speech with Low Speech Distortion Based on Probabilistic Geometric Spectral Subtraction. arXiv: 1802.05125.

[13] Cohen, I. and Berdugo, B. (2001) Speech Enhancement for Non-Stationary Noise Environments. *Signal Processing*, **81**, 2403-2418. https://doi.org/10.1016/s0165-1684(01)00128-1

[14] Wang, Z., Chen, Z., Yu, F. and Liu W. (2004) Warship Noise Measuring and Analyzing. National Defense Industry Press, 148-160.

[15] De Robertis, A., Wilson, C.D., Furnish, S.R. and Dahl, P.H. (2012) Underwater Radiated Noise Measurements of a Noise-Reduced Fisheries Research Vessel. *ICES Journal of Marine Science*, **70**, 480-484. https://doi.org/10.1093/icesjms/fss172

[16] Kim, S.H., Choi, B.K. and Kim, B. (2020) Correlation between Underwater Noise and Sea Level at Ieodo Ocean Research Station. *Journal of Marine Science and Engineering*,

9, Article 1. https://doi.org/10.3390/jmse9010001

[17] Müller, R.A.J., von Benda-Beckmann, A.M., Halvorsen, M.B. and Ainslie, M.A. (2020) Application of Kurtosis to Underwater Sound. *The Journal of the Acoustical Society of America*, **148**, 780-792. https://doi.org/10.1121/10.0001631